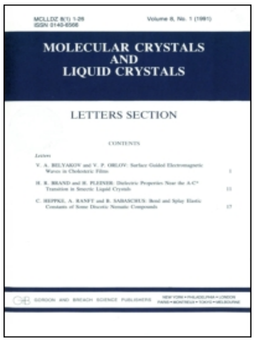

Molecular Crystals and Liquid Crystals

ISSN: 1542-1406 (Print) 1563-5287 (Online) Journal homepage: http://www.tandfonline.com/loi/gmcl20

Effect of radiation on the electrical and luminescent properties of conjugated polymer – porous silicon composite

I. B. Olenych, O. I. Aksimentyeva, L. S. Monastyrskii & O. S. Dzendzeliuk

To cite this article: I. B. Olenych, O. I. Aksimentyeva, L. S. Monastyrskii & O. S. Dzendzeliuk (2016) Effect of radiation on the electrical and luminescent properties of conjugated polymer – porous silicon composite, Molecular Crystals and Liquid Crystals, 640:1, 165-172, DOI: 10.1080/15421406.2016.1257328

To link to this article: http://dx.doi.org/10.1080/15421406.2016.1257328

MOLECULAR CRYSTALS AND LIQUID CRYSTALS
2016, VOL. 640, 165–172
http://dx.doi.org/10.1080/15421406.2016.1257328

Effect of radiation on the electrical and luminescent properties of conjugated polymer – porous silicon composite

I. B. Olenych, O. I. Aksimentyeva, L. S. Monastyrskii, and O. S. Dzendzeliuk

Ivan Franko Lviv National University, Lviv, Ukraine

ABSTRACT

Systematic evaluation of the influence of simultaneous β- and γ-radiation from radium isotope on the electrical and photoluminescent response of hybrid nanocomposites obtained by adding porous silicon nanoparticles into poly(3,4-ethylenedioxythiophene) doped by poly(styrenesulfonate) host matrix is presented. It was found the decrease in the photoluminescence intensity and increasing the electrical conductivity of hybrid film because of radiation exposure. Radiation-induced changes occur in the polymer as well as in PS nanoparticles contributing simultaneously to the total electrical response. The obtained results expand the perspective of nanocomposite applications for radiation sensing.

KEYWORDS

Porous silicon; poly(3,4-ethylenedioxythiophene); nanocomposite; radiation sensing; electrical response

Introduction

The rapid development of nanoelectronics is associated with the search for new functional materials with predictable properties. The composite materials which is a collection of related to each other nanoscale particles allow you to create devices based on them for various purposes: light emitters, photodetectors and electrochemical supercapacitors, chemical and biological sensors [1–4]. Incorporation of the low-dimension components into the conducting polymers, including porous silicon (PS) nanoparticles, allows to maximal use the redox activity of conjugated polymers, size effects and large area surface of nanostructures [5, 6]. Particularly interesting example of a conducting polymer is a poly(3,4-ethylenedioxythiophene) abbreviated hereafter as PEDOT owing to its remarkable optical and electrical properties. The conducting polymers reveal electrical conductivity in the doped states though remains insulators when are undoped (a neutral state). Due to doping-dedoping processes, the electronic properties (e.g., the bandgap) of the conjugated polymers can be varied substantially [7–9].

It is interesting to notice the change of physical properties of the conducting polymers with conjugated backbone and related nanocomposites under the influence of radiation [10–12]. Specific electrical response of polymeric materials makes them good candidates for sensing elements of ionizing radiation. On the other hand, it is worth noting the possibility of modifying the electrical and optical properties of PS as a result of radiation exposure of porous layer [13, 14], the infiltration of nanoparticles of different nature [15, 16] or change the molecular coating of silicon nanocrystals [17, 18]. Probably, one can use porous silicon nanoparticles,

CONTACT I. B. Olenych ✉ iolenych@gmail.com

Color versions of one or more of the figures in the article can be found online at www.tandfonline.com/gmcl.

which have high sensitivity to radiation, for enhancing the performance of sensors. The radiation sensors constructed of these nanocomposites could be made flexible and designed in various geometries to suit the application. Technology their manufacturing is simple and does not require of the expensive materials.

Therefore, a detailed study of particularities of radiation modification of physical parameters of polymeric composites based on PS is relevant and important task as opening the way to creating new types of detectors of ionizing radiation. Present work reports on creating of PEDOT–PS hybrid composites and focuses primarily on the effect of ionizing radiation on electrical and luminescent response of these nanomaterials.

Experiment

To obtain PEDOT-based films an aqueous dispersion of polymeric complex of PEDOT doped by poly(styrenesulfonate) (PSS) is often used. A polymeric anion PSS acts simultaneously as an acid dopant and an anionic surfactant which stabilizes dispersion of the polymer [9, 19]. The hybrid composites were prepared from 1.3% aqueous polymer suspension PEDOT:PSS purchased from Sigma-Aldrich Co, USA.

The other component of our hybrid composite was PS nanoparticles. The PS nanoparticles were prepared using a straightforward procedure of electrochemical etching of single-crystalline silicon n-type conductivity (n-Si), with the specific resistance of 4.5 Ω·cm. Ethanol solution of hydrofluoric acid (the volume ratio of the components HF: $C_2H_5OH = 1{:}1$) was used as an electrolyte. The anodic current density was equal to 40 mA/cm^2 and the etching time was 20 min. To ensure availability of holes in the surface layer of n-Si, which were necessary for occurrence of anodic reactions and formation of the PS, the working surface of a silicon plate was irradiated with white light during the whole process of electrochemical etching [20]. After cleaning of our samples with distilled water and drying in air, a resulting porous layer has been taken off from the surface of the plate. It had the shape of a finely-dispersed powder. The sizes of silicon particle ranged from a few tens of nanometers to several microns.

The PS nanoparticles were mixed with the PEDOT:PSS solution and subjected to ultrasonic processing for 2 h. The suspension thus obtained was deposited onto a glass substrate and then dried at the room temperature during 48 h. Eventually, a monolithic film of the hybrid PEDOT:PSS-PS nanocomposite was obtained. The thickness of the film was about 20 μm. For studying the electrical properties of the hybrid composite films, silver contacts were thermally deposited onto the films surface. The distance between them was about 5 mm, as shown in Fig. 1.

To investigate the influence of the ionizing radiation on the properties of PEDOT:PSS–PS nanocomposites we have used ^{226}Ra isotope with an activity of 0.1 mCi. The decay of ^{226}Ra results in the radiation of γ-rays with an energy of about 0.19 MeV. Produced β-radiation has an average energy of about 0.17 MeV. The experimental samples of PEDOT:PSS–PS were placed at 0.6 m distance from the radiation source. Therefore, there was no need to account for α-particles with energy of 4.78 MeV, which are typically absorbed already after traveling several centimeters in air. Radiation dosage was evaluated considering the exposure time.

The PEDOT:PSS–PS composite was characterized by scanning electron microscopy (SEM) REMMA-102-02 (“Selmi”, Ukraine) and Fourier transform infrared (FTIR) spectroscopy. The transmittance spectra were measured with an “Avatar” spectrometer in the wave number region of 400–4000 cm^{-1}. To obtain the IR spectra of the hybrid films, the composite PEDOT:PSS–PS was deposited, using the method described above, on a silicon wafer with

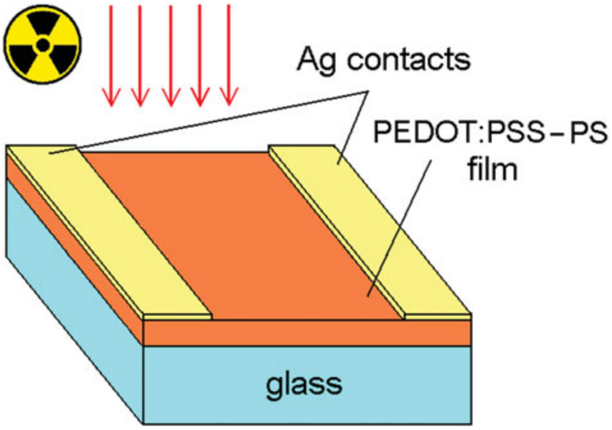

Figure 1. PEDOT:PSS–PS structure with contacts. Arrows show the incoming radiation from ^{226}Ra isotope.

the thickness of 400 μm. The absorption bands of the silicon substrate were easily identified (see [21]). To identify the absorption bands of the PEDOT:PSS–PS films, the literature data [4, 9, 22, 23] may be considered. PL of hybrid films was studied using CM2203 spectrofluorometer ("Solar", Belarus). PL spectra were registered in 450–800 nm range using UV light excitation ($\lambda = 330$ nm) at ambient temperature.

Electrical resistivity measurements at room temperature were performed using E7-20 immitance meter ("Kalibr", Belarus) in the frequency range of 25 Hz–1 MHz. Temperature dependences of electric conductivity were measured in vacuum (10^{-3} mm Hg) starting from liquid nitrogen temperature. Polarization voltage was 5 V. Samples were heated linearly at the rate of 0.1 K/sec.

Results and discussion

Analysis of the surface of the PEDOT:PSS film and PEDOT:PSS–PS hybrid film was carried out using SEM methods in modes of secondary electrons and X-ray microanalysis (EDS). SEM images of the surface of both films are shown in Fig. 2. As one can see from Fig. 2,a, the PEDOT:PSS formed a monolithic polymer film. Study the surfaces of PEDOT:PSS–PS hybrid film exhibit a considerable variation in dispersivity of PS powder, integrated into the polymer film (see Fig. 2,b). The X-ray microanalysis of the hybrid film structures found the traces of silicon and carbon, oxygen and sulfur, which are components of the PEDOT:PSS polymer.

To identify the components of the hybrid systems PEDOT:PSS–PS, we have measured their FTIR spectra (Fig. 3). Most intense are IR bands in the 620–660 cm^{-1} range corresponding to bending Si–H$_2$ mode and the absorption band located at 1100 cm^{-1} that can be related to valence Si–O–Si vibrations of the silicon substrate and PS nanoparticles [21, 22]. The band at 460 cm^{-1} is usually ascribed to deformation vibrations of Si–O group [21]. The absorption bands observed in the FTIR spectra of the PEDOT:PSS–PS composite, which are located in the regions 1080–1310 and 1500–1550 cm^{-1}, are characteristic for C–O, Si–O–C complexes and C = C, C–C vibrations of thiophene rings [9, 23]. Besides, the IR spectra of the hybrid composite include the absorption band with the maximum located at 860 cm^{-1} and the peaks in the regions of 950–1000 cm^{-1}. These bands are characteristic for hydrogen containing molecular complexes: O–SiH$_x$ ($x = 1, 2$) and C–M, respectively [4, 9]. The band at around 2300 cm^{-1} usually corresponds to stretching complexes which include carbon or hydrogen, particularly, carbon dioxide CO$_2$ or O$_3$–Si–H.

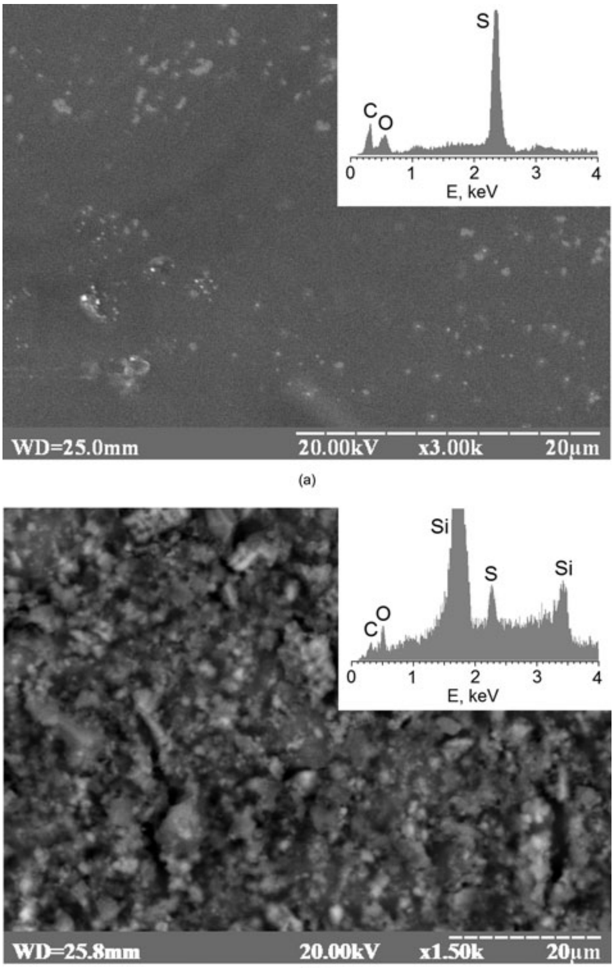

(a)

(b)

Figure 2. SEM image and X-ray microanalysis of the PEDOT:PSS film (a) and PEDOT:PSS–PS composite (b) surfaces.

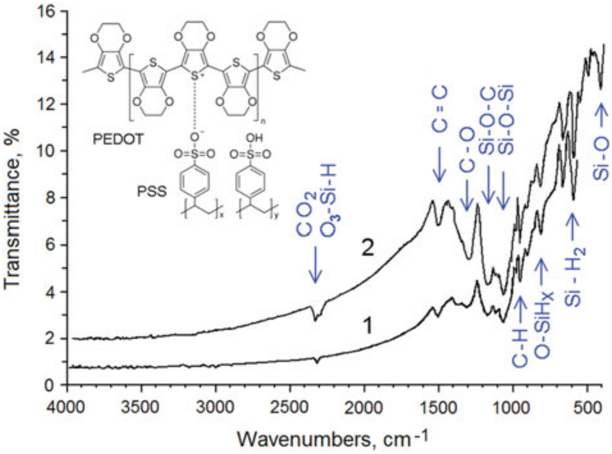

Figure 3. FTIR spectra of hybrid PEDOT:PSS–PS films on the silicon substrate before (1) and after the influence of ionized radiation (2). Inset shows chemical formula of PEDOT:PSS.

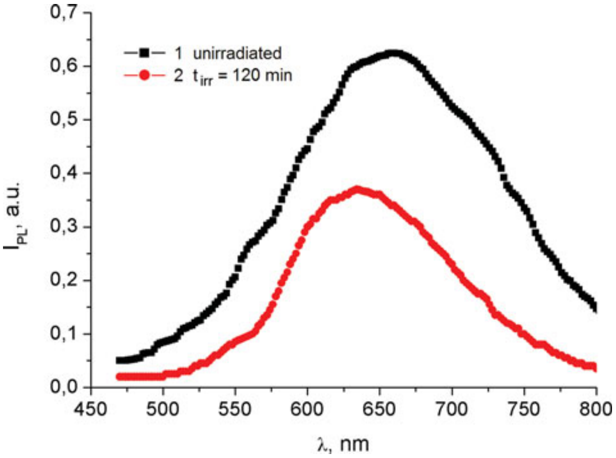

Figure 4. PL spectra of the PEDOT:PSS–PS film before (1) and after the influence of ionized radiation (2).

After 120 min of irradiation from ^{226}Ra source was observed some redistribution of the intensity of IR bands in the ranges 1080–1310 and 1500–1550 cm^{-1}, which could be related to radiation-stimulated concurrent processes of destruction and cross-linking in the polymer and transformation of PS nanoparticles molecular coating, which we attribute to the change in passivation of dangling bonds of PS nanocrystals by both hydrogen and structural components of the polymer.

Fig. 4 shows the PL spectra of the PEDOT:PSS–PS film before and after the influence of β- and γ-radiation from ^{226}Ra source. PL properties of hybrid composite are associated to luminescent nanocrystals of PS. The PS visible PL band is a superposition of emissions resulting from the radiative recombination of electron-hole pairs excited in silicon nanocrystals of various sizes. Their electronic spectrum is modified due to the quantum confinement effect [6, 24]. PL spectra of the PEDOT:PSS–PS hybrid composite contain a broad emission band with a maximum at 630–680 nm for luminescence excitation by UV light with $\lambda = 330$ nm. Since dispersion of PEDOT: PSS has a very weak PL with a maximum about 400 nm [25], the red band of PL of the hybrid composite may be associated with photon emission in PS [14, 24].

Under the influence of irradiation we have observed decrease in the intensity of the visible photoluminescence of PS-based hybrid composite. The PL band maximum is also shifted to higher energies. The emission band width narrowed because the intensity of its long-wavelength tail decreased. Similar changes occur in the PL spectra of PS under the influence of radiation from ^{226}Ra source [14]. These changes could be related to a modification in the surface passivation of luminescent silicon nanocrystals that present by FTIR-spectroscopy data.

Studying the frequency dependence of the electrical resistance of the PEDOT:PPS–PS composite showed decrease in the resistance of experimental samples from 52.3 to 1.3 MΩ as frequency increases from 25 Hz to 1 MHz (Fig. 5). Taking into account that resistance of PEDOT:PPS–PS hybrid composite is higher by three orders for the resistance of the reference PEDOT:PSS sample (with no addition of PS powder) [12], we can assume that electrical properties of composite are more dependent on silicon nanoparticles.

Simultaneous influence of β- and γ-radiation from ^{226}Ra isotope significant decreases the resistance of PEDOT:PSS–PS composite in the 0.025–100 kHz range, as it does in the case of PS structures [14]. The magnitude of resistance change depends on the radiation dosage (see

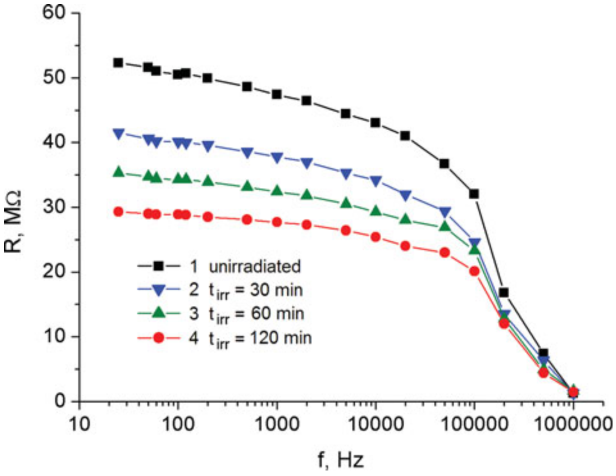

Figure 5. Resistance of hybrid PEDOT:PSS–PS composite as a function of frequency.

Fig. 5). That can be caused by the formation of radiation defects and a built-in charge in PS nanocrystals and radiation induced concurrent processes of destruction and cross-linking in the polymer. Polymer chain break due to absorbed ionizing radiation gets in the way of charge transfer through π- electron conjugations. On the other hand, the appearance of dangling bonds with uncompensated valence electrons allows chain interlocking and stimulates cross-linking of the polymer [12]. In case of the composite the both radiation-induced changes in PS nanoparticles and polymer should be considered.

Temperature dependence of the conductivity of the hybrid PEDOT:PSS–PS films in the temperature range of 80–260 K shows exponential increase of the conductivity with temperature (Fig. 6). This indicates the activation mechanism of charge transfer in structures [26]. Based on the temperature dependence of the resistivity represented in coordinates ln R – 1/T, we can estimate the activation energy of conductivity. Activation energy of conductivity for hybrid films calculated by angle of graphics ln R – 1/T was about 0.07 eV in the low temperature area and 0.25 eV in the 220–260 K range.

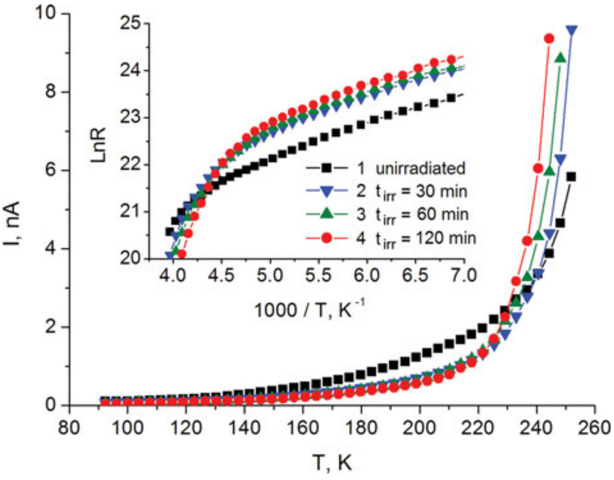

Figure 6. Temperature dependencies of electrical conductivity of hybrid PEDOT:PSS–PS composite. Inset: temperature dependence of the resistivity represented in coordinates ln R – 1/T.

β- and γ-radiation stimulated changes in PEDOT:PSS–PS nanocomposite also affect the temperature dependence of its electrical conductivity. Radiation exposure of hybrid film by ^{226}Ra isotope led to a slight increase in the activation energy of conductivity in the temperature range of 220–260 K. After 120 min of irradiation the activation energy was about 0.42 eV. Radiation-induced changes occur in the polymer as well as in PS nanoparticles contributing simultaneously to the total electrical response.

Conclusions

We have created the PEDOT:PSS–PS composite films for radiation sensors. Using the FTIR and energy-dispersive X-ray spectroscopy, we have determined the components present in the hybrid layer. In particular, it was found the main IR absorption bands related to the structural chains of the polymer and to some interactions of polymer complexes with the PS nanocrystals. Under the influence of simultaneous influence of β- and γ-radiation was observed the change of IR absorption bands intensity and therefore the transformation of PS nanoparticles molecular coating.

The effect of simultaneous β- and γ-radiation from ^{226}Ra source on the luminescent and electrical properties of PS was investigated using comprehensive studies. The experimentally established decrease in the photoluminescence intensity and increasing the electrical conductivity of PEDOT:PSS–PS nanocomposites caused to β- and γ-irradiation. In addition, ionizing radiation causes increase in the activation energy of conductivity in the 220–260 K temperature range. Thus, it was demonstrated that the electrical properties of these composites show high sensitivity to the dosage of β- and γ-radiation. This expands the perspective of new nanotechnological applications of composite material for radiation sensing.

References

[1] Francis, R., Joy, N., Aparna, P., & Vijayan, R. (2014). *Polymer Rev*, *54*, 268–347.

[2] Fung, D. D. S., Qiao, L., Choy, W. C. H., Wang, C., Sha, W. E. I., Xie, F., & He, S. (2011). *J. Mater. Chem.*, *21*, 16349–16356.

[3] Wang, H., Hao, Q., Yang, X., Lu, L., & Wang, X. (2009). *Electrochem. Commun.*, *11*, 1158–1161.

[4] Olenych, I. B., Aksimentyeva, O. I., Monastyrskii, L. S., Horbenko, Y. Y., & Yarytska, L. I. (2015). *Nanoscale Res. Lett.*, *10*, 187.

[5] Aksimentyeva, O. I., Monastyrskyi, L. S., Savchyn, B. M., Stakhira, P. Y., Vertsimakha, Ya. I., & Tsizh, B. R. (2007). *Mol. Cryst. Liq. Cryst.*, *467*, 73–83.

[6] Bisi, O., Ossicini, S., & Pavesi, L. (2000). *Surf. Sci. Rep.*, *38*, 1–126.

[7] Heeger, A. J. (2001). *Synth. Metals*, *125*, 23–42.

[8] Leclere, Ph., Surin, M., Brocorens, P., Cavallini, M., Biscarini, F., & Lazzaroni, R. (2006). *Mater. Sci. Engin. R*, *55*, 1–56.

[9] Pyshkina, O., Kubarkov, A., & Sergeyev, V. (2010). *Mater. Sci. App. Chem.*, *21*, 51–54.

[10] Kane, M. C., Lascola, R. J., & Clark, E. A. (2010). *Radiat. Phys. Chem.*, *79*, 1189–1195.

[11] Tatro, S. R., Clayton, L. M., Muisener, P. A. O., Rao, A. M., & Harmon, J. P. (2004). *Polymer*, *45*, 1971–1979.

[12] Karbovnyk, I., Olenych, I., Aksimentyeva, O., Klym, H., Dzendzelyuk, O., Olenych, Yu., & Hrushetska, O. (2016). *Nanoscale Res. Lett.*, *11*, 84.

[13] Bhave, T. M., Bhoraskar, S. V., Singh, P., & Bhoraskar, V. N. (1997). *Nucl. Instrum. Meth. Phys. Res. B*, *132*, 409–417.

[14] Olenych, I. B., Monastyrskii, L. S., & Dzendzeliuk, O. S. (2015). *Journal of Nano- and Electronic Physics*, *7*, 04063.

[15] Amran, T. S., Hashim, M. R., Al-Obaidi, N. K., Yazid, H., & Adnan, R. (2013). *Nanoscale Res. Lett.*, *8*, 35.

[16] Kim, J., Joo, S. S., Lee, K. W., Kim, J. H., Shin, D. H., Kim, S., & Choi, S.-H. (2014). *ACS Appl. Mater. Interfaces*, *6*, 20880–20886.

[17] Olenych, I. B., Monastyrskii, L. S., Aksimentyeva, O. I., & Sokolovskii, B. S. (2013). *Electron. Mater. Lett.*, *9*, 257–260.

[18] Monastyrskii, L. S., Aksimentyeva, O. I., Olenych, I. B., & Sokolovskii, B. S. (2014). *Mol. Cryst. Liq. Cryst.*, *589*, 124–131.

[19] Ouyanga, J., Xua, Q., Chua, C. W., Yanga, Y., Lib, G., & Shinar, J. (2004). *Polymer*, *45*, 8443–8450.

[20] Cullis, A. G., Canham, L. T., & Calcott, P. D. J. (1997). *J. Appl. Phys.*, *82*, 909–965.

[21] Niwano, M. (1999). *Surf. Sci.*, *427–428*, 199–207.

[22] Borghesi, A., Sassella, A., Pivac, B., & Pavesi, L. (1993). *Sol. St. Commun.*, *87*, 1–4.

[23] Han, M. G., & Foulger, S. H. (2004). *Chem. Commun.*, *19*, 2154–2155.

[24] Canham, L. T. (1990). *Appl. Phys. Lett.*, *57*, 1046–1048.

[25] Dimitriev, O. P., Piryatinski, Yu. P., & Pud, A. A. (2011). *J. Phys. Chem. B*, *115*, 1357–1362.

[26] Mott, N. F., & Davis, E. A. (1979). *Electronic Processes in Non-Crystalline Materials*, Oxford Univ. Press: Oxford, UK.